Role of surface energy and surface reconstructions on the 2D-to-3D growth-mode transition of strained In x Ga 1-x As layers on InP(001)

Michel Gendry, G. Grenet, Y. Robach, P Krapf, L. Porte, G. Hollinger

Role of surface energy and surface reconstructions on the 2D-to-3D growth-mode transition of strained In$_x$Ga$_{1-x}$As layers on InP(001)

M. Gendry, G. Grenet, Y. Robach, P. Krapf, L. Porte, and G. Hollinger

Ecole Centrale de Lyon, Laboratoire d'électronique, LEAME, UMR-CNRS 5512, F-69131 Ecully Cedex, France

We show that the role played by surface energy in the total-energy balance between the initial two-dimensional (2D) state and the final three-dimensional (3D) state is of prime importance to explain morphologies observed during the molecular-beam epitaxy growth of strained materials. This was established by analyzing differences in 2D-3D transition onsets for 2% mismatched In$_x$Ga$_{1-x}$As films grown on InP(001) substrates when changing the mismatch sign (compression or tension), the film doping, and the type of surface stabilization (anion or cation). The 2D-3D onsets were measured by reflection high-energy electron diffraction and the corresponding surface morphologies characterized by scanning tunneling microscopy. [S0163-1829(97)06439-4]

It is now well established that highly mismatched ($>$2%) heteroepitaxy can evolve from a two-dimensional (2D) to a three-dimensional (3D) growth mode before the occurrence of plastic relaxation. Previous experiments[1–3] and models[4–6] revealed that the main parameters controlling the 2D-3D growth mode transition are elastic strain, surface energy, and surface diffusion kinetic. The classical view to explain the 2D-3D growth mode transition is that strained films grow first uniformly and commensurably with the strain energy increasing linearly with thickness up to a critical threshold beyond which it is energetically favorable to form a 3D morphology because of the reduction of the strain energy.

The present work aims to show that surface energy can be, in some cases, the predominant parameter controlling the surface morphology of strained layers and consequently the growth mode. As already emphasized by Tersoff[7] about experiments by Xie *et al.*[8] on Ge$_{0.5}$Si$_{0.5}$/Ge$_x$Si$_{1-x}$/Si(001), any change in the magnitude or sign of the strain can change the surface energies and thus can influence the growth mode. The present paper will evidence the role played by the surface energy when comparing the 2D-3D growth mode transitions and the surface morphologies for 2% mismatched In$_x$Ga$_{1-x}$As films grown on InP(001) by molecular-beam epitaxy (MBE) in different situations: (i) either in compression, viz., $x=0.82$ or in tension, viz., $x=0.25$; (ii) either non-intentionally-doped (nid) or highly doped; and (iii) surfaces either As stabilized or cation stabilized during growth. Experiments were done using reflection high-energy electron diffraction (RHEED) and an ultrahigh-vacuum scanning tunneling microscope (STM).

The samples were grown in a Riber 2300 reactor on well-smoothed In$_{0.53}$Ga$_{0.47}$As buffers (4000 Å) lattice matched to InP(001). The experimental growth conditions as well as the main experimental RHEED results are summarized in Table I. Bragg spot intensities measured during MBE growth for As-stabilized In$_{0.82}$Ga$_{0.18}$As and In$_{0.25}$Ga$_{0.75}$As films using near-equilibrium and far-from-equilibrium growth conditions are shown in Fig. 1. In Table I and Fig. 1, r_{3D} and H_{3D} refer to the critical thickness for the roughening growth mode (weak 2D-3D transition) and for the strong 2D-3D growth

mode transition, respectively. The STM experiments were performed using a Besocke-Beetle ultrahigh-vacuum STM connected to the MBE chamber.[9] Figure 2 shows characteristic images of As-stabilized In$_{0.82}$Ga$_{0.18}$As and In$_{0.25}$Ga$_{0.75}$As strained layers 5 and 13 ML thick, respectively, i.e., just above the corresponding H_{3D} transition. Typical cross sections along the [110] direction are also shown. These STM images are representative of the whole surface, and were obtained with a tunneling current of 0.2 nA and a tunneling voltage of 2 V applied to the sample.[10]

Let us now present and discuss the main RHEED and STM experimental results.

(i) For As-stabilized compressive In$_{0.82}$Ga$_{0.18}$As, the H_{3D} transition that appears around 22 ML with standard growth conditions [Fig. 1(b)], is reduced to 5 ML with near-equilibrium growth conditions [Fig. 1(a)]. In contrast, for As-stabilized tensile In$_{0.25}$Ga$_{0.75}$As, the H_{3D} onset is only slightly reduced from 14 ML with far-from-equilibrium growth conditions [Fig. 1(d)] to 10.5 ML with near-equilibrium growth conditions [Fig. 1(c)]. In the compressive case [Fig. 1(a)], the RHEED Bragg spot intensity remains perfectly constant below the H_{3D} threshold, indicating true or quasitrue 2D growth mode as checked by STM.[10] In contrast, in the tensile case [Fig. 1(c)], a weak and continuous increasing of the RHEED Bragg spot intensity is observed, starting from the early stages of growth beyond a threshold labeled r_{3D}. This phenomenon is associated to an increasing roughening of the surface before the onset of the 3D growth mode. Before and after the 2D-3D transition, a strong (2×4) RHEED pattern is always observed for As-stabilized In$_{0.82}$Ga$_{0.18}$As, even stronger than for lattice-matched As-stabilized In$_{0.53}$Ga$_{0.47}$As, whereas no reconstruction is observed for As-stabilized In$_{0.25}$Ga$_{0.75}$As.

(ii) STM measurements just beyond H_{3D} (Fig. 2), clearly show the growth of highly anisotropic, 5–10 ML high 3D platelets, elongated in the [1$\overline{1}$0] direction for both As-stabilized In$_{0.82}$Ga$_{0.18}$As and As-stabilized In$_{0.25}$Ga$_{0.75}$As. The platelet mean width in the [110] direction is equal to 250 Å for As-stabilized In$_{0.82}$Ga$_{0.18}$As but only equal to 150 Å for As-stabilized In$_{0.25}$Ga$_{0.75}$As. Island cross sections reveal

TABLE I. 2D-3D critical thicknesses (H_{3D}) and roughness critical thicknesses (r_{3D}) in monolayers (ML), and RHEED surface reconstructions as a function of the experimental growth conditions: growth temperature (°C), growth rate (ML s^{-1}), V/III beam-equivalent-pressure (BEP) ratio, for 2% mismatched In$_x$Ga$_{1-x}$As layers on InP(001) near equilibrium and far from equilibrium.

Growth conditions $T = 525°$	Experimental			Compression In$_{0.82}$Ga$_{0.18}$As		Tension In$_{0.25}$Ga$_{0.75}$As	
		Doping	Surface stabilization	2D-3D critical thickness (ML)	RHEED surface reconstruction	2D-3D critical thickness (ML)	RHEED surface reconstruction
Near equilibrium	V/III BEP=70 0.22 ML s^{-1}	NID	As	$H_{3D}=5$	strong (2×4)	$r_{3D}=1-2$ $H_{3D}=10.5$	no
		5×10^{18} cm^{-3}	As	$H_{3D}=3.5$	no	$r_{3D}=1-2$ $H_{3D}=10.5$	no
	V/III BEP=5 0.22 ML s^{-1}	NID	cation	no	strong (4×2)	no	strong (4×2)
Far from equilibrium	V/III BEP=20 0.66 ML s^{-1}	NID	As	$H_{3D}=22$	strong (2×4)	$r_{3D}=2$ $H_{3D}=14$	no
		5×10^{18} cm^{-3}	As	$H_{3D}=5.5$	no	$r_{3D}=2$ $H_{3D}=14$	no
	V/III BEP=5 0.66 ML s^{-1}	NID	cation	no	strong (4×2)	no	strong (4×2)

that a major part of the surface is formed by flat (001) planes (island tops and valley bottoms) that represent about 70% and 50% of the whole surface for As-stabilized In$_{0.82}$Ga$_{0.18}$As and As-stabilized In$_{0.25}$Ga$_{0.75}$As, respectively. In both cases, the side facets form an angle of 17.4° relative to the (001) plane, i.e., close to 19.5° of the (114) plane orientation.[1,11,12]

(iii) In compression, for both near-equilibrium and far-from-equilibrium growth conditions, the critical thickness H_{3D} for As-stabilized layers is strongly reduced from undoped to highly doped samples. In contrast, no difference is observed in tension. This has to be associated to the quality of the RHEED patterns which appear to be different between highly doped and undoped layers in compression whereas no difference is observed in tension.

(iv) Changing the surface reconstruction from (2×4) As-stabilization to (4×2) cation stabilization prevents the 3D growth mode appearing both for tension and compression. With cation-stabilized growth conditions, a strong (4×2) RHEED reconstruction is observed both for compression and tension.

The earliest model that has been evoked to justify a 3D morphology for strained films is the Asaro-Tiller-Grinfeld instability model,[13] which predicts that surface undulations
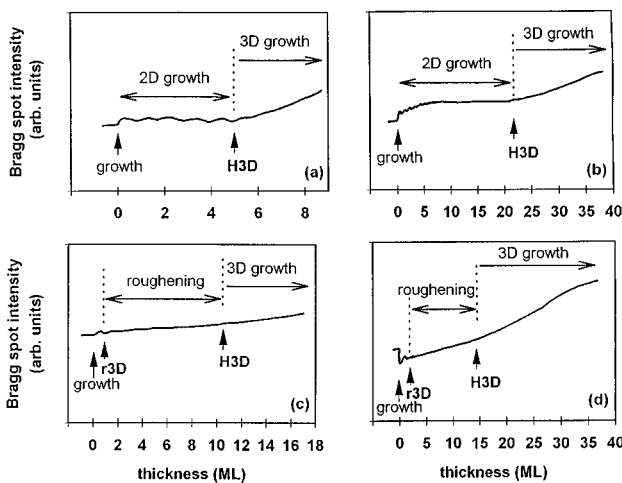

FIG. 1. Bragg spot intensity measured during the growth of As-stabilized (a) In$_{0.82}$Ga$_{0.18}$As using near-equilibrium growth conditions, (b) In$_{0.82}$Ga$_{0.18}$As using far-from-equilibrium growth conditions, (c) In$_{0.25}$Ga$_{0.75}$As using near-equilibrium growth conditions, and (d) In$_{0.25}$Ga$_{0.75}$As using far-from-equilibrium growth conditions. H_{3D} and r_{3D} indicate the onsets of the 3D growth and of the rough growth, respectively.

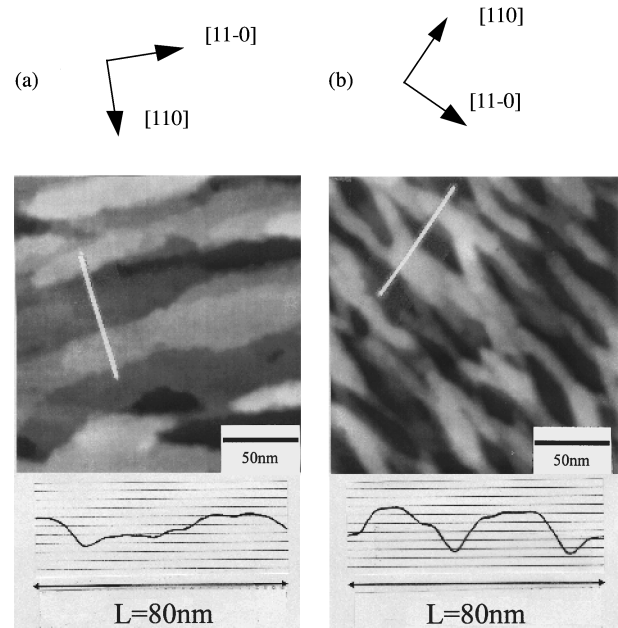FIG. 2. STM images of As-stabilized In$_{0.82}$Ga$_{0.18}$As (a) and In$_{0.25}$Ga$_{0.75}$As (b) strained layers 5 and 13 ML thick, respectively, and corresponding cross sections. Distance between two horizontal lines of the cross section is 5 Å.

can reduce the total energy. However, this continuous model, useful to predict the precursor 2D surface undulations, cannot be invoked when a 2D-3D growth mode transition occurs because it does not take into account the crystal structure and thus the orientation dependence of surface energies. A more recent way[6,7] to predict the 2D-3D growth mode transition is to compare the total energy E_T defined as bulk strain energy E_B plus surface energy E_S, for the two competing 2D and 3D processes: the transition arises when the final 3D state has a total energy $E_T^f = E_B^f + E_s^f$ smaller than that $E_T^i = E_B^i + E_S^i$ of the initial 2D state, taking into account that $E_B^f < E_B^i$, and $E_S^f > E_S^i$. At this stage, it is worth noting that the smaller $E_S^f - E_S^i$ is, the smaller the 2D-3D critical thickness will be and that E_s^f includes contributions both from platelets and facets.

The strain energy density per bulk unit cell in $In_xGa_{1-x}As$ may be calculated from the usual Matthews relationship.[14] We found $E_B = 0.198$ meV per $Å^3$ for $In_{0.82}Ga_{0.18}As$ and $E_B = 0.259$ meV per $Å^3$ for $In_{0.25}Ga_{0.75}As$. On the other hand, the surface energy per surface unit cell is strongly dependent on the reconstructions allowed for the (001) face at a given As coverage θ_{As}. The $In_xGa_{1-x}As(001)$ surface energies are not known; however, relative trends can be predicted using data and results for GaAs surface reconstructions that have been extensively studied.[15-18] For As-stabilized GaAs(001), it has been shown[15] that the surface energy is strongly reduced from 42.7 meV per $Å^2$ for the As-rich unreconstructed surface ($\theta_{AS} = 1$) to 21 meV per $Å^2$ for the (2×4) reconstruction ($\theta_{AS} = 0.75$). Thus, for a few ML coverage, the surface-energy term is about ten times higher than the bulk elastic energy and so a slight variation in surface energy should strongly modify the 2D-3D energy balance. This may explain the observed differences between the compression and tension cases since strain may influence the surface energy as follows: In the (2×4) reconstruction, the As-As dimers are lying above the ideal lattice position by +0.29 Å due to bond relaxation.[15] Considering that the mismatch-induced lattice distortion naturally moves up for compressively strained $In_{0.82}Ga_{0.18}As$ on InP and down for tensilely strained $In_{0.25}Ga_{0.75}As$ on InP, it appears that the surface is better stabilized for compressively strained $In_{0.82}Ga_{0.18}As$ on InP than for lattice-matched $In_{0.53}Ga_{0.47}As$. For the tensilely strained $In_{0.25}Ga_{0.75}As$ on InP, the bond distortion is too great for As dimers to be well stabilized. This favors some disorder and should prevent the (2×4) reconstruction from being well established. Local order should involve As dimers and differences occur only in the amount of long-range disorder that is greater for tension than for compression. This explains the differences in the quality of the reconstruction pattern observed by RHEED (Table I) for As-stabilized $In_xGa_{1-x}As$ layers: a strong (2×4) pattern for compression, a weak (2×1) pattern for lattice matched layers, and no reconstruction for tension. This behavior corresponds to an increase in surface energy from compression to tension.

Beyond the 2D-3D growth mode transition, the 3D morphology (Fig. 2) for both compression and tension is characterized by platelets and valleys made of (001) and (114) planes but with a different size and distributions (see Fig. 2). The similarity between tension and compression 3D morphologies allows us to consider that bulk energies E_B^f should

be slightly identical in compression and tension. On this basis, the differences in 3D onset observed between compression and tension are explained as follows: the strong (2×4) reconstruction in compression (low E_S^i) keeps the surface from roughening until the appearance of a clear 3D growth mode onset because the surface energy in the 3D final state is much higher due to the presence of the (114) facets ($E_S^f - E_S^i$ is large). Conversely, the breaking of the reconstruction in tension allows roughening of the surface even at the early growth stages (r_{3D}). This can be understood because the energy of a disordered 2D surface is high and close to that of a rough surface ($E_S^f - E_S^i$ is small). In fact, the presence of many single steps as on a rough surface implies also a breaking of the (2×4) reconstruction. In this case, the roughening thus allowed permits, in its turn, the strain energy to be partially relaxed and consequently delays the formation of large islands (H_{3D}) unlike the compressive case. As discussed above, the surface energy of tensilely strained $In_xGa_{1-x}As$ is higher than that of the corresponding relaxed material. This suggests that this effect could be the reason for the formation of small islands that relax strain more efficiently than larger ones. In compression, island tops tend to be as large and as flat as possible to preserve the best long-range order for the initial strong (2×4) reconstruction. Note that our explanation (surface modification) about the origin of the difference of surface roughness between compression and tension is similar to that given by Tersoff.[7] However, there is no discrepancy with the arguments of Xie et al.[8] since changes in surface energy through roughness are directly related to the number and the type of the existing steps. The difference observed between our $Ga_xIn_{1-x}As$ surface (tensile layer rougher than compressive layer) and the Xie et al. SiGe surface (compressive layer rougher than tensile layer) arise probably because the III-V zinc-blende semiconductor involves two kinds of atoms (anions plus cations) whereas diamondlike compounds involve only one.

The role of surface reconstruction effects has been confirmed by experimental results obtained for highly doped As-stabilized samples. Doping is known to weaken the reconstruction long-range order: the surface generally presents domain boundaries between well-reconstructed regions,[18] which increases the surface energy. In compression, the 2D-3D growth mode onset occurs earlier for highly doped samples than for unintentionally doped samples due to reduced $E_S^f - E_S^i$. In tension, since no reconstruction is detected by RHEED, doping cannot affect strongly the surface reconstruction nor the surface energy and thus the 2D-3D growth-mode-transition onset is not doping dependent since $E_S^f - E_S^i$ remains constant.

No 2D-3D transition is observed for the cation-stabilized growth mode either for compression or for tension. The hierarchy between surface tensions versus surface orientation[17] allows in some cases a facetting of the initial (001) face into (111) facets, and thus into (114)A facets made in our case from (001) plus (111)A planes (as double A steps). For GaAs(001), the cation-rich (4×2) reconstructed (001) surfaces are known to have a higher surface energy (38.4 meV per $Å^2$) than the (2×4) As-stabilized (001) ones (21 meV per $Å^2$).[15] For GaAs(111)A, the surface energy is 58.4–68.9 meV per $Å^2$ for the As-stabilized (111)A surface

orientation but 134.6–144.4 meV per $Å^2$ for the Ga-stabilized $(111)A$ surface orientation.[17] This suggests that In-rich $(114)A$ facets made of In-rich (001) and $(111)A$ planes should have a very high surface energy and consequently a low probability to exist. In contrast, As-rich $(114)A$ facets have a lower surface energy. This explains why a 2D-3D growth mode transition occurs in As-rich conditions and not in In-rich conditions (large $E_S^f - E_S^i$).

In summary, we have shown that when minimizing kinetic effects by using near-equilibrium growth conditions, the surface energy through surface reconstructions can be a preponderant parameter in determining the onset of the 2D-3D growth mode transition and the resulting 3D morphology. Because the As-terminated (001) surface may be strongly stabilized if reconstructed by surface dimers, any effect that modifies the long-range ordering of this reconstruction (as doping may do) or its efficiency (as strain may do) will affect the 2D-3D growth-mode-transition onset, all thing being equal in the final state. However, in tension, the breaking of the surface reconstruction allows a roughening of the surface that partially relaxes the strain energy and thus delays the strong 2D-3D growth mode transition. On the other hand, changing growth conditions, from As stabilization to cation stabilization, prevent a 3D growth mode because facetting of the (001) face into $(114)A$ plans is energetically allowed only if the surface is As stabilized during growth.

[1] G. J. Whaley and P. I. Cohen, in *Layered Structures: Heteroepitaxy, Superlattices, Strain, and Metastability*, edited by B. W. Dodson, L. W. Showalter, J. E. Cunningham, and F. H. Pollak, MRS Symposia Proceedings No. 160 (Materials Research Society, Pittsburgh, 1990), p. 35; Appl. Phys. Lett. **57**, 144 (1990).

[2] C. W. Snyder *et al.*, Appl. Phys. Lett. **66**, 3032 (1991); C. W. Snyder, J. M. Manfield, and B. G. Orr, Phys. Rev. B **46**, 9551 (1992); C. W. Snyder, H. Muneka, and B. G. Orr, Appl. Phys. Lett. **62**, 46 (1993); C. W. Snyder and B. G. Orr, *ibid.* **62**, 46 (1993).

[3] N. Grandjean, J. Massies, and V. H. Etgens, Phys. Rev. Lett. **69**, 796 (1992).

[4] B. J. Orr *et al.*, Europhys. Lett. **19**, 33 (1992).

[5] J. Tersoff and R. M. Tromp, Phys. Rev. Lett. **70**, 2782 (1993); J. Tersoff and F. K. LeGoues, *ibid.* **72**, 3570 (1994).

[6] C. Priester and M. Lannoo, Phys. Rev. Lett. **75**, 93 (1995).

[7] J. Tersoff, Phys. Rev. Lett. **74**, 4962 (1995).

[8] Y. H. Xie *et al.*, Phys. Rev. Lett. **73**, 3006 (1994); **74**, 4963 (1995).

[9] P. Krapf, J. P. Lainé, Y. Robach, and L. Porte, J. Phys. III **5**, 1871 (1995).

[10] L. Porte *et al.*, Surf. Sci. **352/354**, 60 (1996); P. Krapf, Y. Robach, M. Gendry, and L. Porte, Phys. Rev. B **55**, 10 229 (1997).

[11] G. Hollinger *et al.*, Appl. Phys. Lett. **57**, 144 (1992).

[12] A. Ponchet *et al.*, J. Cryst. Growth **153**, 71 (1995).

[13] X. Asaro and Y. Tiller, Metall. Trans. **13**, 1789 (1972); M. A. Grinfeld, J. Intell. Mater. Syst. Struct. **4**, 76 (1993).

[14] J. W. Matthews, J. Vac. Sci. Technol. **12**, 126 (1975).

[15] Guo-Xin Qian, R. M. Martin, and D. J. Chadi, Phys. Rev. B **37**, 1303 (1988); **38**, 7649 (1988); Phys. Rev. Lett. **60**, 19 (1988).

[16] E. Kaxiras *et al.*, Phys. Rev. B **35**, 9625 (1987); **35**, 9636 (1987).

[17] N. Chetty and R. M. Martin, Phys. Rev. B **45**, 6089 (1992).

[18] M. D. Pashley, Phys. Rev. B **40**, 10 481 (1989); M. D. Pashley, K. W. Haberern, and R. M. Feenstra, J. Vac. Sci. Technol. B **10**, 1874 (1992); M. D. Pashley and K. W. Haberen, Ultramicroscopy **42**, 1281 (1992).